Brain, Behavior, & Immunity - Health 18 (2021) 100376

Contents lists available at ScienceDirect

Brain, Behavior, & Immunity - Health

journal homepage: www.editorialmanager.com/bbih/default.aspx

Using quantitative MRI to study brain responses to immune challenge with interferon-α

Maria Antonietta Nettis [a,b,*,1], Andrew J. Lawrence [a,b,1], Tobias Wood [c], Nicole Mariani [a], Naghmeh Nikkheslat [a], Giulia Lombardo [a], Daniela Enache [d], Mattia Veronese [b,c], Federico E. Turkheimer [c], Paola Dazzan [a,b], Carmine M. Pariante [a,b], Valeria Mondelli [a,b]

[a] King's College London, Institute of Psychiatry, Psychology and Neuroscience, Department of Psychological Medicine, London, UK
[b] National Institute for Health Research Mental Health Biomedical Research Centre, South London and Maudsley NHS Foundation Trust and King's College London, London, UK
[c] King's College London, Institute of Psychiatry, Psychology and Neuroscience, Department of Neuroimaging, London, UK
[d] Karolinska Institute, Department of Neurobiology, Care Sciences and Society, Division of Neurogeriatrics, Stockholm, Sweden

ARTICLE INFO

Keywords:
Neuroinflammation
MRI
Quantitative relaxometry
Interferon-α
Depression

ABSTRACT

Inflammatory processes in the Central Nervous System (CNS) have been proposed to mediate the association between peripheral inflammation and the development of psychiatric disorders, but we currently lack sensitive measures of CNS inflammation for human studies *in vivo*. Here we used quantitative MRI (qMRI) to explore the *in vivo* central response to a peripheral immune challenge in healthy humans, and we assessed whether changes in quantitative relaxometry MRI parameters were associated with changes in peripheral inflammation.

Quantitative relaxation times (T1 & T2) and Proton Density (PD) were measured in n = 6 healthy males (mean age = 30.5 ± 6.8 years) in two MRI assessments collected before and 24 hours after a subcutaneous injection of the proinflammatory cytokine and immune activator, interferon-alpha (IFN-α). Serum levels of immune markers and markers of blood-brain barrier integrity (S100B) were also measured before and after the injection.

Region of interest and histogram-based analyses (optimized for the small sample size) showed a statistically significant increase of both T1 ($t_{(5)} = 3.78$, $p = 0.013$) and PD ($t_{(5)} = 2.91$, $p = 0.033$) parameters in the bilateral hippocampus after IFN-α administration. T1 peak values in bilateral hippocampus were positively correlated with serum Tumour Necrosis Factor-alpha levels at 24 h after the injection, when this cytokine peaked (Spearman's rho = 0.67, p = 0.018) and negatively correlated with S100B levels (Spearman's rho = −0.826, p = 0.001).

Our data suggest that peripheral administration of IFN-α produces acute changes in brain qMRI which might indicate a brain immune response. This is supported by the association of such changes with low-grade peripheral inflammation.

1. Introduction

Inflammation in the Central Nervous System (CNS) has been proposed to play an important role in the development of psychiatric disorders, possibly through its effects on neurogenesis and neuroplasticity (Baumeister et al., 2014; Enache et al., 2019). However, measuring neuroinflammatory processes in humans *in vivo* has proven extremely challenging, particularly considering that the levels of peripheral or central inflammation in patients with psychiatric disorders are not as high as during infection or other immunological disorders. Positron Emission Tomography (PET) has been used to measure central inflammation in a number of recent studies on both healthy subjects and patients with depression, mainly focussing on the expression of translocator protein (TSPO) which has been suggested to represent a marker of microglia activation (Mondelli et al., 2017). However, this technique is expensive, invasive and has a number of methodological limitations, as our group has shown in a recent study (Nettis et al., 2020). Overall, PET studies conducted so far indicated the presence of a modest TSPO increase in depressed patients compared with healthy subjects (Schubert

* Corresponding author. G.33.81 The Maurice Wohl Institute of Neuroscience, Institute of Psychiatry, Psychology and Neuroscience, King's College, London, Cutcombe road, SE59RT, London, UK.
E-mail address: maria.a.nettis@kcl.ac.uk (M.A. Nettis).
[1] Joint first authors.

https://doi.org/10.1016/j.bbih.2021.100376
Received 30 September 2021; Accepted 18 October 2021
Available online 19 October 2021

Abbreviations

BBB	blood-brain barrier
IFN-α	interferon-alpha
IL	interleukin
MS	multiple sclerosis
nPD	normalised proton density
PD	proton density
rACC	rostral anterior cingulate cortex
ROI	region of interest
TNF-α	tumour necrosis factor-alpha
TSPO	translocator protein
VEGF-A	vascular endothelial factor-A

et al., 2020), but the majority of these studies did not find a correlation between peripheral and central inflammation (Nettis et al., 2020).

Magnetic Resonance Imaging (MRI) techniques have several advantages over PET: they are widely available; do not require the use of radioactive ligands and are therefore safer for repeated scanning studies; and are considerably less expensive. MRI offers enormous potential for indirect *in vivo* study of neuroinflammatory processes, in particular through high resolution quantitative MRI methods (qMRI) which can infer tissue microstructural properties (Alexander et al., 2019; Deoni, 2010; Wang et al., 2015). Specifically, quantitative relaxometry parameters reflect brain free water content and the amount of CNS tissue components (e.g., cells, myelin, lipids, proteins). Thus, they can be informative of disease-related tissue changes, developmental plasticity, and other biological processes, including inflammation (Deoni, 2010).

Relaxometry has been mainly used to measure white matter microstructure and demyelination; indeed, changes of relaxometry parameters have been detected in patients affected by multiple sclerosis (MS) and Alzheimer disease (Deoni, 2010), both characterized by genuine neuroinflammatory processes. Only recently, the potential application of this MRI technique in disorders with a less clear neuroinflammatory signature, such as psychiatric disorders, has started to be implemented (Cookey et al., 2018; Vanes et al., 2018).

However, such studies can be affected by the intrinsic heterogeneity of the clinical population (i.e., stage of the disorder, medication use, age). That is why models in healthy humans are crucial to validate new methods for measuring neuroinflammatory processes and dissecting their biological components.

In this pilot study, we used qMRI in healthy humans to study the central response to the immune challenge interferon-alpha (IFN-α), the most validated clinical model of inflammation-induced depression (Raison et al., 2006; Hepgul et al., 2010). This included a pre-, and a 24-h-post–IFN–α, PET scan with [^{11}C]PBR28, in seven subjects, with the aim of measuring direct signs of neuroinflammation in terms of microglial activation (Nettis et al., 2020). We based the study design on a pre-clinical study showing that in vitro IFN-α-stimulated microglia release inflammatory cytokines after approximately 24 h (Zheng et al., 2015). Interestingly, our PET results showed no changes in PET signal measures. This suggested either that there was no microglial activation in our acute model or that the radioligand was not sensitive enough to measure TSPO upregulation.

In the present study, we sought to explore the presence of a central response to IFN-α administration, in the same sample of subjects, with MRI relaxometry. In particular, we aimed to establish whether IFN-α-induced peripheral inflammation was associated with changes in MRI relaxometry parameters in 5 regions of interest: the cerebral white matter (i) the bilateral hippocampus (ii) the bilateral amygdala (iii), the anterior cingulate cortex (iv), and cerebral cortical ribbon (v).

As secondary aims, we also explored 1) the association between changes in levels of peripheral cytokines and qMRI measures after IFN-α administration and 2) the association between markers of blood-brain barrier (BBB) permeability and measures of both peripheral and central inflammation. This is because in-vitro and preclinical models showed that systemic inflammation is associated with BBB disruption and increased permeability (Hsuchou et al., 2012). Therefore, we wanted to explore whether changes in the BBB permeability were associated with the immune signal from the body to the brain.

2. Methods

2.1. Participants

We recruited seven healthy males for this study through local and media advertisement. Given the small sample size, we recruited only male participants to avoid the confounding effect of gender. Male subjects were preferred, so that women in their fertile age would not be exposed to interferon administration.

Only one subject was excluded from the analysis due to methodological reasons (described below). In order to determine eligibility, participants had a pre-screening phone call, followed by a screening visit. Their medical history was collected, and a MINI Psychiatric scale administered. Eligible participants were non-smokers, drank no more than five alcohol drinks per week, had no history of significant medical illness and did not meet the criteria for any current or past psychiatric or substance-dependence diagnosis. Subjects were excluded if they had had an infection in the last month, had regularly used anti-inflammatory drugs or had contraindications to MRI scanning. Subjects were also instructed to abstain from alcohol, anti-inflammatory medication and physical exercise for 72 h before the scans.

Participants' consent was obtained according to the Declaration of Helsinki prior to enrolment in the study and all procedures were approved by the Queen Square London Ethical committee (Reference 16/LO/1520). Sociodemographic characteristics are shown in Table 1.

After the screening visit, participants returned for visits on two consecutive days. On day 1, they had the baseline MRI scan (A session) at 9AM, followed by subcutaneous injection of IFN-α (2a Roferon-A 3 million IU/0.5 ml solution for injection). Participants were monitored for side effects for 8 h after the injection and then discharged home. In order to closely monitor changes in peripheral inflammatory markers, blood samples were collected 1 h before and at 2, 4 and 6 h after IFN-α administration. The day after (day 2), again at 9AM, participants came back to have the 24 h post–IFN–α MRI (B session), followed by blood sample collection. All participants had their MRIs at 9 AM with approximately 24 h between A and B session. One participant had his B session 6 months after the A session, but still 24 h after the IFN-α injection and he was included in the analysis.

2.2. MRI imaging procedures

MRI scans were obtained on a 3 T General Electric Healthcare MR 750 scanner at the Institute of Psychiatry, Psychology and Neuroscience, King's College London. Each session lasted 60 min. A T1-weighted Inversion Recovery Gradient Echo scan was acquired with 0.9 mm isotropic voxels, TR 8.2 ms, Flip-Angle 12° and TI 450 ms.

The relaxometry protocol consisted of axially oriented Spoiled

Table 1
Sociodemographic data.

Subjects	Age	Ethnicity	BMI
01	28	Black-African	20.38
02	25	Black-African	23.12
03	33	Asian-Filippino	24.54
04	43	Black-African	24.68
05	29	White-British	23.62
06	25	Mixed	22.24
Mean ± SD	30.50 ± 6.80	–	23.09

Gradient Recalled echo (SPGR) (Flip-Angles 1.5, 3, 10 & 20°, TE/TR 4.8/10.6 ms) and Steady State Free Procession (SSFP) (Flip-Angles 12 & 50°, TR 5.6 ms, phase-increments 45, 135, 225 & 315°) scans acquired with 1.2 mm isotropic voxel size. We acquired four SPGR images at different flip-angles and a total of eight SSFP images (two flip-angles at four phase-increments). A Bloch-Siegert map was acquired for B1 inhomogeneity correction (Sacolick et al., 2010). One subject from the original seven was excluded because a B1 map from one session was missing.

2.3. Data processing and analysis

Due to the small sample size, and potential for spatially heterogenous effects, we did not conduct a traditional voxel-wise analysis. Instead, we looked at histograms of the qMRI measures and their change between timepoints within a-priori brain regions (ROIs). We plotted histograms, but primarily analysed measures of the average change over the voxels within the region of interest (ROI) defined for each subject. We term this a histogram/ROI-analysis.

For this analysis, we selected five bilateral a-priori ROIs: (i) cerebral white matter; (ii) the bilateral hippocampus; (iii) the bilateral amygdala; (iv) the bilateral rostral anterior cingulate cortex (rACC) and (v) a wider cortical ribbon area which included regions (ii-iv). As mentioned in the introduction, microstructure changes in the white matter, in terms of myelin alterations, have already been detected with relaxometry in neuroimmune diseases like MS (Deoni, 2010), so we selected the white matter ROI as we expected microstructural differences to be apparent here. Moreover, the hippocampus, the amygdala and the anterior cingulate cortex are gray matter areas that have been specifically involved in the neurobiology of immune-related depression (Kim and Won, 2017). Finally, we included the cortical ribbon in order to detect overall gray matter changes and to compare them with specific changes in the hippocampus, amygdala and ACC.

All ROIs were produced by Freesurfer with Desikan-Killiany-Tourville (DKT) (Klein and Tourville, 2012) parcellation used for the bilateral rACC and hippocampus ROIs.

2.4. MRI pre-processing

T1, T2 and Proton Density (PD) maps were processed using the Joint-System Relaxometry approach (Teixeira et al., 2018) implemented within the Quantitative Imaging Tools (QUIT) toolbox (Wood et al., 2016) (https://github.com/spinicist/QUIT). Of note, the Joint Relaxometry fitting method comes from a family of similar methods (often referred to as DESPOT1/DESPOT2 or the VFA method) that have been the subject of comprehensive literature (Deoni et al., 2003, 2004; Jutras et al., 2016; Deoni, 2007, 2009).

For each subject, the MRI relaxometry data were rigidly registered to the anatomical T1-weighted (T1w) image and the higher resolution images were then used for within and between subject co-registration, tissue classification and ROI identification via anatomical atlas. Prior to analysis, the apparent PD maps were bias corrected and rescaled to make the average intensity of cerebrospinal fluid signal within the lateral ventricles equal to one. We henceforth refer to these maps as normalised PD (nPD) (Tustison et al., 2010).

Anatomical T1w images from the A session (pre–IFN–α) and B session (post–IFN–α) were processed with the longitudinal Freesurfer stream (Reuter et al., 2012). This includes a robust, inverse consistent registration that produces an unbiased within-subject mid-space template. In general, this template is used to improve the accuracy of longitudinal MR processing, increasing reliability and statistical power (Reuter et al., 2012). ROI/histogram analysis was conducted after transforming images from template space to subject specific mid-space.

2.5. Subtraction images

For each quantitative (q) MRI measure (T1, T2, and nPD) subtraction images were created in the Freesurfer subject-specific longitudinal mid-space. Each qMRI map was transformed in a single concatenated step to minimise interpolation effects. Once in the mid-space, session A values were subtracted from session B. Thus, a positive voxel in the subtraction image indicates a positive effect of IFN-α on the qMRI measure, and contrarywise for negative voxels.

2.6. ROI analysis

For each ROI, a bilateral binary mask was extracted based on the processing of the participant's unbiased-mid-space image. For each qMRI measure (T1, T2, nPD) the mask was applied, and basic statistics (mean, median) calculated. Then, measure-specific range limits were applied, and histogram of distribution obtained. Bin-widths varied dependent on the ROI used. Histogram bin frequencies were normalised to the total number of voxels in the ROI and the maximum normalised frequency used to calculate the Peak Location (or Peak Value) and its Normalised Peak Height (NPH). Whole tissue class ROIs (white matter and cortical ribbon) contained 50–100 times more voxels than the smaller gray matter ROIs (Hippocampus/Amygdala/rACC) and so a larger number of bins (i.e., smaller bin width) were used for the physically larger regions (750 vs. 75 bins for the GM ROIs). All histograms were inspected to confirm the distribution was unimodal, the limits did not exclude voxels, and the peak was well described by the Peak Location/NPH.

2.7. Peripheral inflammatory biomarkers

Serum levels of interferon (IFN)-γ, interleukin (IL)-1β, IL2, IL-4, IL6, IL-8, IL-10, IL12p70, IL-13, tumor necrosis factor (TNF)-α, vascular endothelial growth factor (VEGF)-A were measured using Meso Scale Discovery (MSD) V-PLEX sandwich immunoassays, and plates read on an MSD QuickPlex SQ 120, as in a previous study conducted in our laboratory (Nettis et al., 2020).

MSD Pro-inflammatory Panel 1 (human) kit was used for the measurement of IFN-γ, IL-1β, IL-2, IL-4, IL-6, IL-8, IL-10, IL-12p70, IL-13, and TNF-α, and a custom Cytokine Panel 1 (human) kit was used for the measurement of vascular endothelial growth factor VEGF-A. The inter-assay coefficient of variations was <10%. The results were analysed using MSD DISCOVERY WORKBENCH analysis software. All samples were analysed in duplicates and the mean value was used as a final result.

Serum levels of high sensitivity C-reactive protein (hsCRP) were assayed on the Siemens Advia 24000 Chemistry analyzer (Siemens Healthcare Diagnostics, Frimley, UK) (Mason et al., 2013).

2.8. Markers of Blood Brain Barrier (BBB) integrity

Serum levels of S100B, as a biomarker of BBB integrity (Argaw et al., 2012), were analysed on the Liaison XL chemiluminescence analyses (Nettis et al., 2020). A number of studies have used S100B as a non-invasive marker of BBB integrity. Indeed, increased serum S100B has been used as evidence of BBB disruption in seizures (Marchi et al., 2007), exercise and hyperthermia (Watson et al., 2005), sepsis (Larsson et al., 2005), brain ischemia during carotid artery cross clamping for carotid endarterectomy (Jaranyi et al., 2003) and traumatic brain injury (Blyth et al., 2009).

2.9. Statistical analysis

For the ROI/histogram-based analysis, we were interested in the typical change of the voxels within the ROI. Of note, histogram analysis proved to be useful in comparable types of quantitative MRI imaging, such as diffusion imaging (Downey et al., 2013). As the distribution of change over the voxels is unknown, we considered three measures of central tendency: the mean, median and histogram mode (or peak). These values were each assessed for statistical significance against the null hypothesis (qMRIB – qMRIA = 0) with one-sample t-tests

(uncorrected for multiple comparisons). Particularly, we considered that effects driven by extreme changes in a small number of voxels might only be present in the mean, while the median would not show this influence of extreme values but would be affected by asymmetry about the mode. The histogram peak location would be unaffected by asymmetry or extreme values. We considered as significant only findings that were consistently significant across the three measures of central tendency: peak value, mean and median.

For statistical analysis, the effect size was calculated as Hedges' G. The equation used for Hedges' G calculation employed the approximation for the correction factor provided in the original work from Hedges (1981).

Cytokines and hsCRP values were log transformed. Two-tailed Spearman's correlations were performed to explore the association between MRI changes and markers of BBB integrity and peripheral inflammatory markers that peaked at 24 h post-administration of IFN-α (at the same time of the second MRI scan). Peripheral inflammatory markers that peaked at 24 h included TNF-α, IL-8 and hsCRP, as previously described (Nettis et al., 2020).

3. Results

3.1. Quantitative relaxometry

3.1.1. Bilateral hippocampus

The ROI/histogram analysis showed that both T1 and nPD increased, in a statistically significant way, in the bilateral hippocampus ROI, following the immune challenge. This was indicated by the histograms of the distribution of the subtraction image (B – A) (Fig. 1), following calculation of the maps of qMRI for the two sessions. These effects were also present when a non-parametric Wilcoxon test was used.

The qMRI findings for the histogram peak value for each ROI are described in Table 2. Of note, for both T1 and nPD in the bilateral hippocampus, the peak value of the difference (B-A) histogram of T1 was statistically significantly greater than 0 (Table 2). This result was consistent across all the employed measures of central tendency (histogram peak value, mean, median), as shown in Fig. 2. Standardised effect sizes and statistical hypothesis test results for all ROIs are also displayed in Fig. 2.

3.1.2. Other areas

We found a significant effect for mean T1 in the cortical ribbon ROI ($t_{(5)} = 2.78$, $p = 0.038$, $W = 21$, $p = 0.03125$, Hedges' G of 0.95). However, the increase was not significant for the median or peak value measures, so it was not consistent across different measures of central tendency (Fig. 2).

Although non-significant, the general pattern in the amygdala and the white matter was towards increases in T1 and nPD with a less reliable and smaller decrease in T2 for the white matter.

In contrast with results in other areas, the bilateral rostral anterior cingulate cortex (rACC) showed an opposite direction, with decreased T1 values (peak values of B-A histogram) (average over the subject: -0.012, $t_{(5)} = -1.9$, $p = 0.11$).

3.1.3. Correlation of MRI measures with markers of BBB integrity and peripheral inflammatory biomarkers

Two-tailed Spearman's correlations were performed to explore the association between MRI measures and the three peripheral inflammatory markers that peaked at 24 h post-administration of IFN-α (at the same time of the second MRI scan), that is, TNF-a, IL-8 and hsCRP (Nettis et al., 2020). We also explored association with S100B levels. The

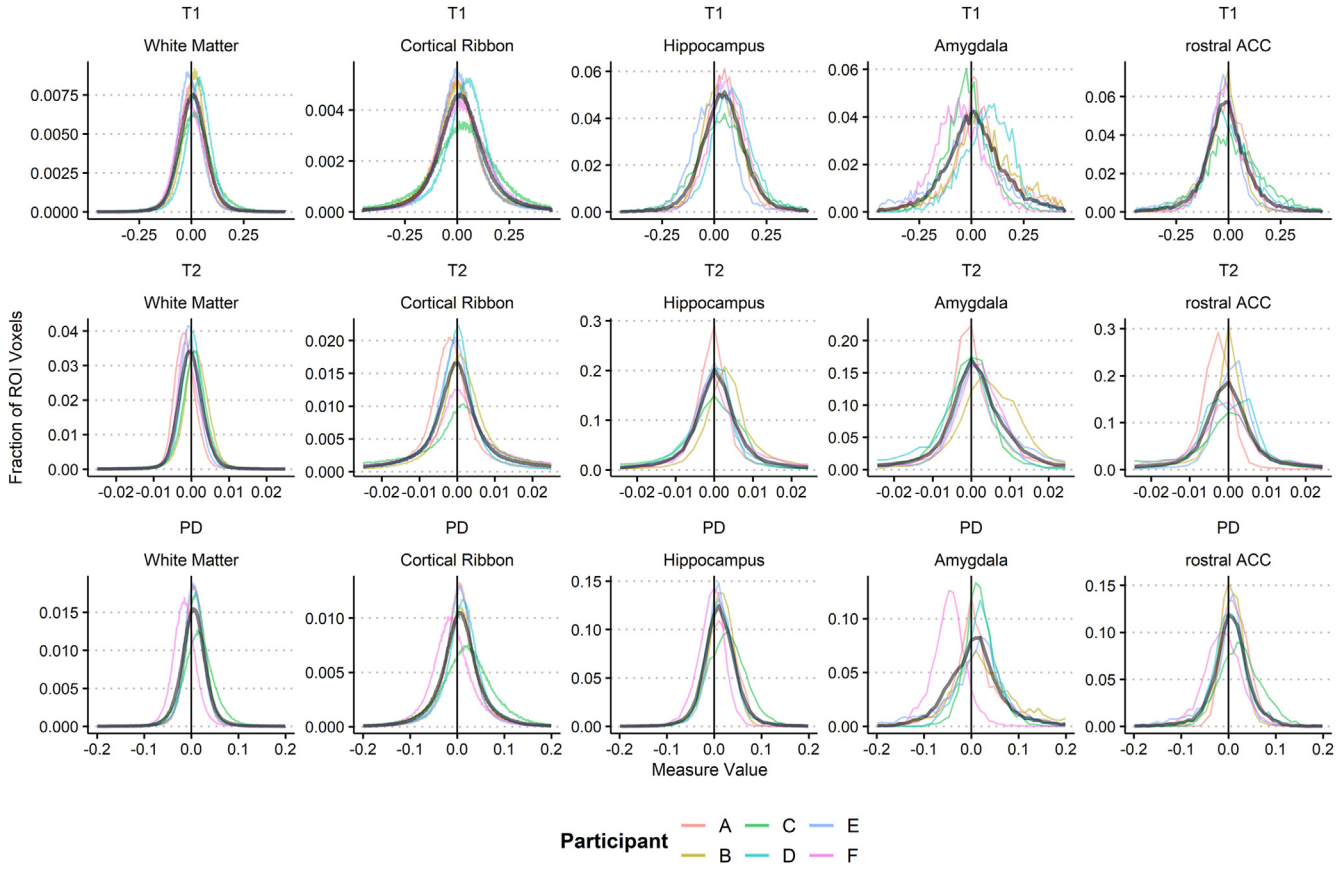

Fig. 1. Histograms of Session B - Session A. Normalised histograms of difference image values (Session B Session A) are displayed for different Regions of Interest (rows) and qMRI measures (columns). Subject-level histograms are displayed in colour, while the black line shows the group average histogram. (For interpretation of the references to colour in this figure legend, the reader is referred to the Web version of this article.)

Table 2
Histogram peak value results across ROIs.

	Modality	Average over the subject	95% CI	Statistics		Hedge's G
				parametric	Non-parametric	
Hippo	**T1**	0.040	+0.013 – +0.068	$t_{(5)} = 3.78, p = 0.013$*	W = 21, p = 0.036*	1.299
	T2	0.0004	−0.0007 – +0.002	$t_{(5)} = 1.00$, p = 0.36	W = 1, p = 1.0	0.343
	nPD	0.011	0.001 – +0.021	$t_{(5)} = 2.91, p = 0.033$*	W = 15, p = 0.048*	0.999
rACC	**T1**	−0.012	−0.028 – +0.004	$t_{(5)} = -1.93$, p = 0.11	W = 0, p = 0.18	−0.666
	T2	0.0009	−0.002 – +0.004	$t_{(5)} = 0.79$, p = 0.46	W = 5, p = 0.42	0.272
	nPD	0.003	−0.007 – +0.013	$t_{(5)} = 0.79$, p = 0.46	W = 5, p = 0.42	0.272
Ctx	**T1**	0.009	−0.009 – +0.028	$t_{(5)} = 1.31$, p = 0.25	W = 17, p = 0.22	0.449
	T2	0	−0.001 – +0.001	$t_{(5)} = 0$, p = 1	W = 11.5, p = 0.92	0
	nPD	0.005	−0.009 – +0.019	$t_{(5)} = 0.93$, p = 0.39	W = 16, p = 0.31	0.321
Amyg	**T1**	0.010	−0.049 – +0.070	$t_{(5)} = 0.43$, p = 0.68	W = 9, p = 0.79	0.149
	T2	0.0009	−0.006, – +0.0002	$t_{(5)} = 1.58$, p = 0.17	W = 3, p = 0.34	0.543
	nPD	0.0001	−0.0245– +0.028	$t_{(5)} = 0.15$, p = 0.88	W = 10, p = 0.59	0.053
WM	**T1**	0.006	−0.019– +0.031	$t_{(5)} = 0.59$, p = 0.58	W = 12, p = 0.84	0.205
	T2	−0.0005	−0.002 – +0.0008	$t_{(5)} = -0.98$, p = 0.37	W = 6, 0.40	−0.336
	nPD	0.004	−0.006 – +0.014	$t_{(5)} = 0.99$, p = 0.37	W = 15, p = 0.44	0.341

Hippo = hippocampus.
rACC = rostral Cingulate Cortex.
Ctx = cortical ribbon.
Amyg = amygdala.
WM = white matter.
nPD = normalised proton density.

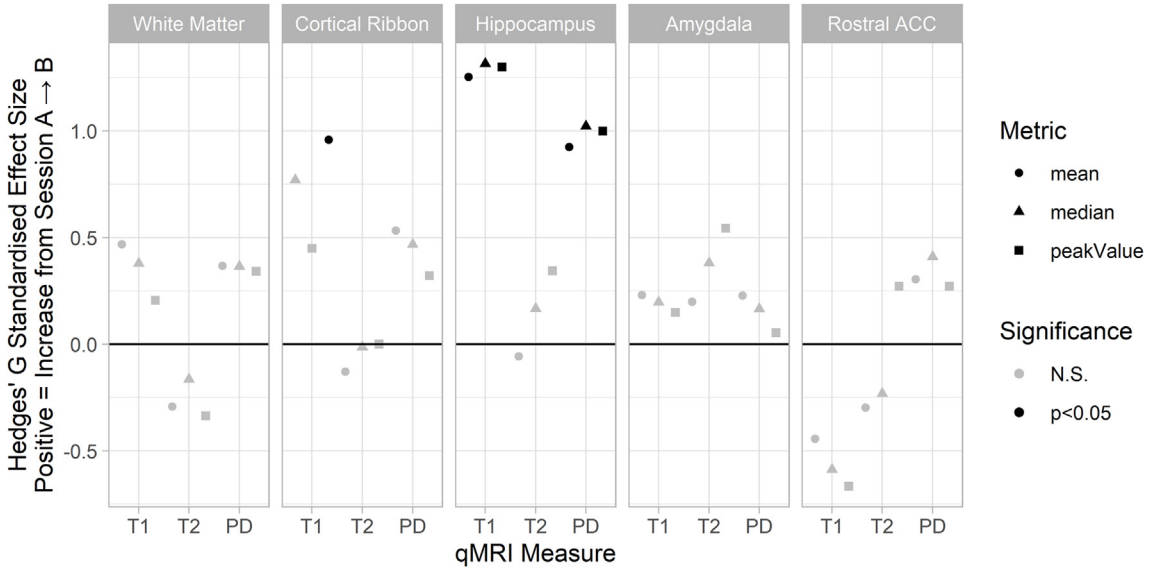

Fig. 2. Effects of Immune Challenge on qMRI. Standardised effect size for change between session A and session B are presented for measures of the central tendency of the qMRI difference images: mean, median, and histogram peak (circles, triangles & squares respectively). Hypothesis test results from one-sample t-tests are indicated by colour. Panels show different regions of interest: WM = cerebral white matter, ctx = cerebral cortical ribbon, hippo = bilateral hippocampal cortex, rACC = bilateral rostral Anterior Cingulate Cortex.

correlations included values of both baseline and 24 h after IFN-α. We found that T1 peak values in bilateral hippocampus were positively correlated with TNF-a levels (Spearman's rho = 0.67, p = 0.018) and negatively correlated with S100B values (Spearman's rho = −0.826, p = 0.001). Overlapping results were found when using T1 mean and median values for both TNF-α (Spearman's rho = 0.69, p = 0.013; Spearman's rho = 0.76, p = 0.004, respectively) and for S100B (Spearman's rho = −0.59, p = 0.044; Spearman's rho = −0.68, p = 0.014, respectively). Of note, S100B values were unchanged at 24 h after the challenge. However, when looking at the overall curve of this marker, we found a downward trajectory in the first 4 h after IFN-α, as described in Fig. 3 (Wilcoxon test for S100B between 1 h before and 4 h after IFN-α = -2.02, p = 0.04).

4. Discussion

The present study assesses, for the first time, MRI high-resolution relaxometry brain response to acute IFN-α administration in healthy humans. We find that relaxometry parameters change following the administration of IFN-α, that such changes are localized in the hippocampus and are correlated with low-grade peripheral inflammation.

Previous imaging studies have reported associations between pro-inflammatory states and functional and structural alterations in this brain region, which is involved in emotional regulation (Mondelli et al., 2011; Marsland et al., 2008). Indeed, alterations in structure and function of the hippocampus due to the neurotoxic effects of increased inflammation have been associated with the pathophysiology of depression

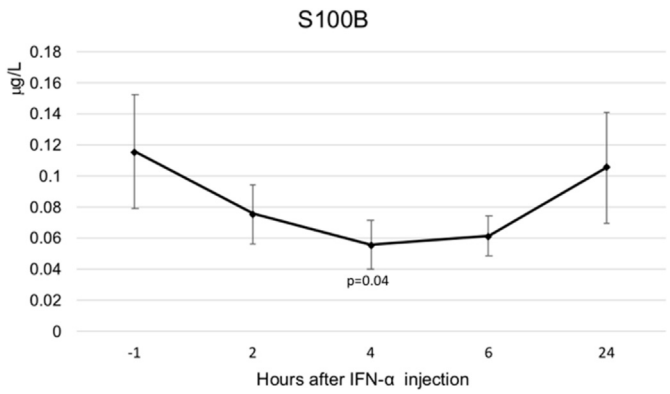

Fig. 3. S100B levels from 1 h before IFN-α administration to 24 h after. Wilcoxon test between 1 h before and 4 h after IFN-α =-2.02, p=0.04.

(Kim and Won, 2017). However, relaxometry reflects changes in tissue density or chemical composition, so it can add sensitivity to volumetric MRI and detect abnormalities not observed in conventional imaging (Vos et al., 2020).

Our main result is the increased value of T1 and nPD in the bilateral hippocampus following administration of IFN-α. This result was consistently significant across different employed measures of central tendency: histogram peak value, mean and median.

T1 is influenced by the relative amount of non-water CNS tissue components (cells, myelin, lipids, proteins), by water content, and dissolved oxygen. Thus, increased T1 can indicate decreased CNS tissue "structure" (loss of cells, axons, myelin) (Albrecht et al., 2016) and it has proven useful in evaluating oedema in the brain (i.e. inflammatory oedema) (Albrecht et al., 2012; Downey et al., 2013).

Previous pre-clinical studies have focussed on the influence of demyelination on T1, but such models have usually been affected by a certain degree of inflammation, so that the specific contribution of different processes (demyelination vs inflammation) to the signal cannot be disentangled (Wood et al., 2016; O'Muircheartaigh et al., 2019). NPD maps measure the amount of free water protons, and this measure appears to have a linear relationship with T1 measures (Mezer et al., 2013). However, its pathophysiological interpretation remains uncertain.

As mentioned in the introduction, this study was part of a research including pre- and post–IFN–α PET scans with [11C]PBR28 in the same subjects, showing no changes in PET signal measures. However, our MRI results suggest that some alterations were present in the brain at 24 h after the challenge (mirrored by peripheral increases in inflammatory biomarkers) and that MRI was sensitive enough to detect them. We interpret these alterations as the consequence of underlying neuroinflammatory processes induced by the IFN-α administration. Moreover, considering that TSPO-PET, targeting intracellular alterations like gliosis, showed negative results, it is conceivable that MRI changes reflected reactions in the extracellular compartment.

Supporting the link between our quantitative MRI parameters and central inflammatory processes, we also found a correlation between such parameters and some peripheral inflammatory markers. This was surprising, as studies of PET-measured neuroinflammation in psychiatric disorders have often been unsuccessful in finding such associations, albeit with some exceptions (Attwells et al., 2020), possibly because the magnitude of these associations, if present, is smaller than that present in pure neuroinflammatory conditions, such as acute endotoxemia or neurodegenerative disorders (Notter et al., 2018).

Our study was undoubtedly limited by the small sample size. In order to draw further conclusions, our findings should be replicated in larger samples of healthy humans and include measures of diffusion tensor imaging and free tissue water fraction to better understand whether the MRI changes we identified reflect reactions in the extracellular compartment. Moreover, our within-subjects design relies on the baseline scans as control scans. Thus, the lack of an un-medicated control group in our study limited our ability to control our two-measurement effect. However, the strength of our study is the human model of acute inflammation in healthy subjects, that does not present with the confounding features typical of clinical samples. Overall, we provide preliminary evidence of qMRI potential to measure inflammation-related tissue and water changes in humans in a non-invasive and cost-effective way.

Funding

This paper represents independent research funded by the National Institute for Health Research (NIHR) Biomedical Research Centre at South London and Maudsley NHS Foundation Trust and King's College London. The views expressed are those of the author(s) and not necessarily those of the NHS, the NIHR or the Department of Health and Social Care. This study was supported by Janssen Pharmaceutical Companies of Johnson&Johnson. This work was also supported by the Wellcome Trust strategy award to the Neuroimmunology of Mood Disorders and Alzheimer's Disease (NIMA) Consortium (104025), which is also funded by Janssen, GlaxoSmithKline, Lundbeck and Pfizer. Dr Mondelli is also funded by MQ: Transforming Mental Health (Grant: MQBF1) and by the Medical Research Foundation (Grant: MRF-160-0005-ELP-MONDE).

Declaration of competing interest

C.M.P. and V.M. have received research funding from Janssen Pharmaceutical NV/Janssen Pharmaceutical, Companies of JohnsonJohnson, partly also contributing to this study. C.M.P. has received research funding from the Medical Research Council (UK) and the Wellcome Trust for research on depression and inflammation as part of two large consortia that also include Johnson & Johnson, GSK and Lundbeck. M.A.N. has received honorarium for speaking from Janssen in one occasion.

Acknowledgments

All IFN-α visits took place at the Clinical Research Facility of King's College Hospital. We would like to thank all the participants in the study. We thank the team of nurses, in particular the Lead Experimental Research Nurse, Noah Yogo, for providing their valuable expertise to the study. We also thank Dr Ottavia Dipasquale for her contribution in the MRI analysis. Finally, we thank the team of radiographers at the Centre for Neuroimaging Sciences of the Institute of Psychiatry, Psychology and Neuroscience, King's College London.

References

Albrecht, S., Eisenblatter, M., Wachsmuth, L., Vogl, T., Faber, C., Kuhlmann, T., 2012. Specific in vivo imaging of inflammation, de-and remyelination using fluorescence molecular tomography. Mult. Scler. J. 18, 389-389.

Albrecht, D.S., Granziera, C., Hooker, J.M., Loggia, M.L., 2016. In vivo imaging of human neuroinflammation. ACS Chem. Neurosci. 7 (4), 470–483. https://doi.org/10.1021/acschemneuro.6b00056.

Alexander, D.C., Dyrby, T.B., Nilsson, M., Zhang, H., Apr 2019. Imaging brain microstructure with diffusion MRI: practicality and applications. NMR Biomed. 32 (4), e3841. https://doi.org/10.1002/nbm.3841.

Argaw, A.T., Asp, L., Zhang, J., et al., 2012. Astrocyte-derived VEGF-A drives blood-brain barrier disruption in CNS inflammatory disease. J. Clin. Invest. 122 (7), 2454–2468. https://doi.org/10.1172/JCI60842.

Attwells, S., Setiawan, E., Wilson, A.A., et al., May 2020. Replicating predictive serum correlates of greater translocator protein distribution volume in brain. Neuropsychopharmacology 45 (6), 925–931. https://doi.org/10.1038/s41386-019-0561-y.

Baumeister, D., Russell, A., Pariante, C.M., Mondelli, V., 2014. Inflammatory biomarker profiles of mental disorders and their relation to clinical, social and lifestyle factors. Soc. Psychiatr. Psychiatr. Epidemiol. 49 (6), 841–849. https://doi.org/10.1007/s00127-014-0887-z.

Blyth, B.J., Farhavar, A., Gee, C., et al., 2009. Validation of serum markers for blood-brain barrier disruption in traumatic brain injury. J. Neurotrauma 26 (9), 1497–1507. https://doi.org/10.1089/neu.2008-073810.1089/neu.2008.0738.

Cookey, J., Crocker, C.E., Bernier, D., et al., 2018. Microstructural findings in white matter associated with cannabis and alcohol use in early-phase psychosis: a diffusion

tensor imaging and relaxometry study. Brain. Connect. 8 (9), 567–576. https://doi.org/10.1089/brain.2018.0611.
Deoni, S.C., Oct 2007. High-resolution T1 mapping of the brain at 3T with driven equilibrium single pulse observation of T1 with high-speed incorporation of RF field inhomogeneities (DESPOT1-HIFI). J. Magn. Reson. Imag. 26 (4), 1106–1111. https://doi.org/10.1002/jmri.21130.
Deoni, S.C., Aug 2009. Transverse relaxation time (T2) mapping in the brain with off-resonance correction using phase-cycled steady-state free precession imaging. J. Magn. Reson. Imag. 30 (2), 411–417. https://doi.org/10.1002/jmri.21849.
Deoni, S.C., 2010. Quantitative relaxometry of the brain. Top Magn. Reson. Imag. 21 (2), 101–113. https://doi.org/10.1097/RMR.0b013e31821e56d8.
Deoni, S.C., Rutt, B.K., Peters, T.M., 2003. Rapid combined T1 and T2 mapping using gradient recalled acquisition in the steady state. Magn. Reson. Med. 49 (3), 515–526. https://doi.org/10.1002/mrm.10407.
Deoni, S.C., Ward, H.A., Peters, T.M., Rutt, B.K., 2004. Rapid T2 estimation with phase-cycled variable nutation steady-state free precession. Magn. Reson. Med. 52 (2), 435–439. https://doi.org/10.1002/mrm.20159.
Downey, K., Riches, S.F., Morgan, V.A., et al., 2013. Relationship between imaging biomarkers of stage I cervical cancer and poor-prognosis histologic features: quantitative histogram analysis of diffusion-weighted MR images. AJR Am. J. Roentgenol. 200 (2), 314–320. https://doi.org/10.2214/AJR.12.9545.
Enache, D., Pariante, C.M., Mondelli, V., Oct 2019. Markers of central inflammation in major depressive disorder: a systematic review and meta-analysis of studies examining cerebrospinal fluid, positron emission tomography and post-mortem brain tissue. Brain Behav. Immun. 81, 24–40. https://doi.org/10.1016/j.bbi.2019.06.015.
Hedges, 1981. Distribution theory for glass's estimator of effect size and related estimators. J. Educ. Stat. 6 (2), 107–128. https://www.jstor.org/stable/1164588.
Hepgul, N., Mondelli, V., Pariante, C.M., Apr-Jun 2010. Psychological and biological mechanisms of cytokine induced depression. Epidemiol. Psichiatr. Soc. 19 (2), 98–102.
Hsuchou, H., Kastin, A.J., Mishra, P.K., Pan, W., 2012. C-reactive protein increases BBB permeability: implications for obesity and neuroinflammation. Cell. Physiol. Biochem. 30 (5), 1109–1119. https://doi.org/10.1159/000343302.
Jaranyi, Z., Szekely, M., Bobek, I., Galfy, I., Geller, L., Selmeci, L., 2003. Impairment of blood-brain barrier integrity during carotid surgery as assessed by serum S-100B protein concentrations. Clin. Chem. Lab. Med. 41 (10), 1320–1322. https://doi.org/10.1515/CCLM.2003.201.
Jutras, J.D., Wachowicz, K., De Zanche, N., Dec 2016. Analytical corrections of banding artifacts in driven equilibrium single pulse observation of T2 (DESPOT2). Magn. Reson. Med. 76 (6), 1790–1804. https://doi.org/10.1002/mrm.26074.
Kim, Y.K., Won, E., Jun 30 2017. The influence of stress on neuroinflammation and alterations in brain structure and function in major depressive disorder. Behav. Brain Res. 329, 6–11. https://doi.org/10.1016/j.bbr.2017.04.020.
Klein, A., Tourville, J., 2012. 101 labeled brain images and a consistent human cortical labeling protocol. Front. Neurosci. 6, 171. https://doi.org/10.3389/fnins.2012.00171.
Larsson, A., Lipcsey, M., Sjolin, J., Hansson, L.O., Eriksson, M.B., 2005. Slight increase of serum S-100B during porcine endotoxemic shock may indicate blood-brain barrier damage. Anesth. Analog. 101 (5), 1465–1469. https://doi.org/10.1213/01.ANE.0000180193.29655.6A.
Marchi, N., Angelov, L., Masaryk, T., et al., 2007. Seizure-promoting effect of blood-brain barrier disruption. Epilepsia 48 (4), 732–742. https://doi.org/10.1111/j.1528-1167.2007.00988.x.
Marsland, A.L., Gianaros, P.J., Abramowitch, S.M., Manuck, S.B., Hariri, A.R., Sep 15 2008. Interleukin-6 covaries inversely with hippocampal grey matter volume in middle-aged adults. Biol. Psychiatr. 64 (6), 484–490. https://doi.org/10.1016/j.biopsych.2008.04.016.
Mason, J.M., Hancock, H.C., Close, H., et al., 2013. Utility of biomarkers in the differential diagnosis of heart failure in older people: findings from the heart failure in care homes (HFinCH) diagnostic accuracy study. PLoS One 8 (1), e53560. https://doi.org/10.1371/journal.pone.0053560.
Mezer, A., Yeatman, J.D., Stikov, N., et al., 2013. Quantifying the local tissue volume and composition in individual brains with magnetic resonance imaging. Nat. Med. 19 (12), 1667–1672. https://doi.org/10.1038/nm.3390.
Mondelli, V., Cattaneo, A., Murri, M.B., et al., Dec 2011. Stress and inflammation reduce brain-derived neurotrophic factor expression in first-episode psychosis: a pathway to smaller hippocampal volume. J. Clin. Psychiatr. 72 (12), 1677–1684. https://doi.org/10.4088/JCP.10m06745.
Mondelli, V., Vernon, A.C., Turkheimer, F., Dazzan, P., Pariante, C.M., 2017. Brain microglia in psychiatric disorders. Lancet Psychiatry. 4 (7), 563–572. https://doi.org/10.1016/S2215-0366(17)30101-3.
Nettis, M.A., Veronese, M., Nikkheslat, N., et al., Mar 9 2020. PET imaging shows no changes in TSPO brain density after IFN-alpha immune challenge in healthy human volunteers. Transl. Psychiatr. 10 (1), 89. https://doi.org/10.1038/s41398-020-0768-z.
Notter, T., Coughlin, J.M., Sawa, A., Meyer, U., 2018. Reconceptualization of translocator protein as a biomarker of neuroinflammation in psychiatry. Mol. Psychiatr. 23 (1), 36–47. https://doi.org/10.1038/mp.2017.232.
O'Muircheartaigh, J., Vavasour, I., Ljungberg, E., et al., May 2019. Quantitative neuroimaging measures of myelin in the healthy brain and in multiple sclerosis. Hum. Brain Mapp. 40 (7), 2104–2116. https://doi.org/10.1002/hbm.24510.
Raison, C.L., Capuron, L., Miller, A.H., 2006. Cytokines sing the blues: inflammation and the pathogenesis of depression. Trends Immunol. 27 (1), 24–31. https://doi.org/10.1016/j.it.2005.11.006.
Reuter, M., Schmansky, N.J., Rosas, H.D., Fischl, B., Jul 16 2012. Within-subject template estimation for unbiased longitudinal image analysis. Neuroimage 61 (4), 1402–1418. https://doi.org/10.1016/j.neuroimage.2012.02.084.
Sacolick, L.I., Wiesinger, F., Hancu, I., Vogel, M.W., May 2010. B1 mapping by Bloch-Siegert shift. Magn. Reson. Med. 63 (5), 1315–1322. https://doi.org/10.1002/mrm.22357.
Schubert, J., Veronese, M., Fryer, T.D., et al., 2020. A modest increase in 11C-PK11195-PET TSPO binding in depression is not associated with serum C-reactive protein or body mass index. medRxiv. https://doi.org/10.1101/2020.06.04.20099556, 2020.06.04.20099556.
Teixeira, R., Malik, S.J., Hajnal, J.V., 2018. Joint system relaxometry (JSR) and Cramer-Rao lower bound optimization of sequence parameters: a framework for enhanced precision of DESPOT T1 and T2 estimation. Magn. Reson. Med. 79 (1), 234–245. https://doi.org/10.1002/mrm.26670.
Tustison, N.J., Avants, B.B., Cook, P.A., et al., 2010. N4ITK: improved N3 bias correction. IEEE Trans. Med. Imag. 29 (6), 1310–1320. https://doi.org/10.1109/TMI.2010.2046908.
Vanes, L.D., Mouchlianitis, E., Wood, T.C., Shergill, S.S., 2018. White matter changes in treatment refractory schizophrenia: does cognitive control and myelination matter? Neuroimage Clin. 18, 186–191. https://doi.org/10.1016/j.nicl.2018.01.010.
Vos, S.B., Winston, G.P., Goodkin, O., et al., 2020. Hippocampal profiling: localized magnetic resonance imaging volumetry and T2 relaxometry for hippocampal sclerosis. Epilepsia 61 (2), 297–309. https://doi.org/10.1111/epi.16416.
Wang, Y., Sun, P., Wang, Q., et al., 2015. Differentiation and quantification of inflammation, demyelination and axon injury or loss in multiple sclerosis. Brain 138 (Pt 5), 1223–1238. https://doi.org/10.1093/brain/awv046.
Watson, P., Shirreffs, S.M., Maughan, R.J., 2005. Blood-brain barrier integrity may be threatened by exercise in a warm environment. Am. J. Physiol. Regul. Integr. Comp. Physiol. 288 (6), R1689–R1694. https://doi.org/10.1152/ajpregu.00676.2004.
Wood, T.C., Simmons, C., Hurley, S.A., et al., 2016. Whole-brain ex-vivo quantitative MRI of the cuprizone mouse model. PeerJ 4, e2632. https://doi.org/10.7717/peerj.2632.
Zheng, L.S., Kaneko, N., Sawamoto, K., 2015. Front. Cell. Neurosci. 9, 5. https://doi.org/10.3389/fncel.2015.00005.